Indian Journal of Pure & Applied Physics
Vol. 53, March 2015, pp. 169-174

Behaviour of acoustical phonons in CeAs in low temperature region

Devraj Singh[1,*], Vyoma Bhalla[1,2], Raj Kumar[3] & Sudhanshu Tripathi[4]

[1]Department of Applied Physics, Amity School of Engineering and Technology, Bijwasan, New Delhi 110 061, India

[2]Amity Institute of Applied Sciences, Amity University, Uttar Pradesh, Noida 201 303, India

[3]Department of Physics, Gurgaon Institute of Technology and Management, Bilaspur-Tauru Road, Gurgaon 122 413, India

[4]Department of Instrumentation and Control Engineering, Amity School of Engineering and Technology, Bijwasan, New Delhi 110 061, India

*E-mail: dsingh13@amity.edu, ultrasonic.devraj@gmail.com

Received 19 May 2014; revised 5 January 2015; accepted 22 January 2015

The ultrasonic attenuation of cerium arsenide (CeAs) has been investigated due to electron-phonon interaction (EPI) in the temperature range 10-70 K at magnetic fields 0-15T along <100>, <110> and <111> directions. The second order elastic constants (SOECs) have also been evaluated using Coulomb and Born-Mayer potentials up to second nearest neighbourhood for the computation of ultrasonic properties like ultrasonic velocity and ultrasonic attenuation. The behaviour of ultrasonic attenuation is reciprocal to resistivity for the magnetic fields 0-15T. The nature of attenuation in CeAs is similar to metals, alkali metals and semi-metallics. It is observed that ultrasonic attenuation due to EPI is most significant at 30 K for all the magnetic fields. The available theoretical evidences support the obtained results.

Keywords: Semi-metallic**,** Electron-phonon interaction, Elastic properties, Ultrasonic properties

1 Introduction

Ultrasonic attenuation measurement and evaluation play an important role in material characterization[1-5]. It helps in providing insight into the microstructure and associated physical properties such as thermal conductivity, specific heat, higher order elastic constants etc., existence of phase transition which gives rise to elastic variation and prediction about the future performance of materials. The wave velocity obtained using elastic constants is a key parameter in ultrasonic characterization and can provide information about crystallographic texture and helps further in the determination of Debye temperature. From the calculated elastic constants, we can also compute the mechanical properties such as Poisson ratio, anisotropic ratio etc. The rare-earth monopnictides with rocksalt structure (B1) have attracted many experimental and theoretical interests due to the presence of strongly correlated f-electrons. The strongly-correlated materials display a great sensitivity to changes in an applied magnetic field. The resistivity over a temperature range 10-70 K could be suppressed to relatively smaller values by the application of magnetic field (*H*). Such properties make the prospect for developing application for correlated materials exciting.

The nature of these f-electrons changes due to change in the physical and chemical properties of these materials under pressure[6,7]. These rare-earth monopnictides are suitable for industrial applications because of their unusual structural, electronic and high pressure properties. CeAs is quite interesting because of its attractive anomalous physical properties. Semi-metallics have attracted much attention since last fifty years [8-13] because of typical low carrier strongly correlated systems with simple rock-salt crystal structure[14, 15]. Hullinger and Ott[8] characterized CeAs single crystal by low temperature measurements of the specific heat, thermal expansion, electrical resistivity and magnetization. The crystal field splitting and magnetic ordering properties of CeAs were observed by Rainford *et al*[9]. using neutron inelastic scattering and power diffraction techniques. Werner *et al*[10]. determined the pressure-volume relationship for CeAs up to a pressure of 32 GPa using energy dispersive XRD. The electronic structure of CeAs including CeN, CeP, CeSb and CeBi have been computed within the self interaction correlated (SIC) local-spin-density (LSD) approximation by Svane *et al*[11]. Mori *et al*[12]. measured electrical resistance of CeAs at different temperature under hydrostatic pressure. Nimori *et al*[13]. studied the

Shubnikov-de Haas (SdH) effect of a CeAs crystal in high magnetic field up to 260kOe. Mori *et al*[14]. investigated the effects of pressure on the electrical and magnetic properties of CeAs. Thompson *et al*[15]. presented a comparison between the pressure dependence of electrical and magnetic properties of anomalous rare-earth and actinide compounds (Ce, Yb and U) that exhibit heavy-fermion and related behaviour. Srivastava *et al*[16]. studied the high pressure phase transition and elastic properties of CeAs using modified interionic potential theory taking into account the Vander Walls interactions.

Few studies on structural and other physical properties exist in literature[8-16]. The major findings are based on the investigation of high-pressure structural phase transition[17]. The grounds mentioned above stimulate us to choose CeAs characterization through ultrasonic evaluations. The ultrasonic attenuation due to EPI for longitudinal and shear modes of propagation along <100>, <110> and <111> directions has been computed in the temperature range 10-70 K using ultrasonic velocities for longitudinal and shear modes of wave propagation and SOECs. In the present paper, a thorough analysis of the relative importance of electron-phonon process[18-20] in determining the low temperature behaviour of the ultrasonic attenuation and electrical resistivity of CeAs is presented.

2 Theory

At low temperatures and high frequencies, the wavelength of ultrasonic wave is comparable to electron mean free path. Thus, coupling between acoustical phonons and conduction electrons causes some loss of energy, and is represented as loss[19] due to EPI. The propagation of longitudinal ultrasonic wave transforms the spherical nature of Fermi surface for an electron gas in equilibrium into an ellipsoid[20] with minor axis along the direction of compression. The electron collision within lattice tends to restore the spherical shape through relaxation phenomenon. The viscous medium plays a vital role in carrying the energy of electrons in normal state to and fro the lattice vibrations. The energy loss results in ultrasonic attenuation due to shear and compressional viscosities[21] are given by:

$$\left(\alpha/f^2\right)_L (\text{Nepers/cm}) = \frac{2\pi^2}{\rho V_L^3}\left(\frac{4}{3}\eta_e + \chi\right) \qquad \ldots(1)$$

and

$$\left(\alpha/f^2\right)_S (\text{Nepers/cm}) = \frac{2\pi^2}{\rho V_S^3}\eta_e \qquad \ldots(2)$$

where η_e is the electron viscosity and is given by:

$$\eta_e(poise) = \frac{9\times10^{11}\hbar^2(3\pi^2 N)^{2/3}}{5e^2 R} \qquad \ldots(3)$$

and ρ is the density of CeAs (2.56 g/cm^3), f the frequency of ultrasonic wave, χ (poise) the compressional viscosity (zero in our case), V_L and V_S are the longitudinal and shear wave velocities (cm/s), N be the number of electrons per unit volume, $\hbar$ is Planck's constant divided by 2π (cm^{2}g/s), e the electronic charge (esu) and R is the electrical resistivity of the chosen CeAs (Ω cm). V_L and V_S are directly related to SOECs along <100>, <110> and <111> directions and are given in literature[22,23].

The SOECs are evaluated using Coulomb and Born-Mayer potential model up to second nearest neighbourhood and is written as:

$$\phi(R) = \phi(C) + \phi(B) \qquad \ldots(4)$$

where $\phi(C)$ is the Coulomb potential (electrostatic) and $\phi(B)$ is the Born-Mayer potential (repulsive). $\phi(C)$ and $\phi(B)$ can be expressed as given below:

$$\phi(C) = \pm\frac{e^2}{r_0} \text{ and } \phi(B) = A\exp\left(-\frac{r_0}{b}\right) \qquad \ldots(5)$$

where r_0 is the nearest neighbour distance; b the hardness parameter, A is the strength parameter. SOECs are obtained following Brugger's definition[24] of elastic constants. According to lattice dynamics which is developed by Leibfried and Ludwig[25], lattice energy changes with temperature. Hence, adding vibrational energy contribution to the static elastic constant (at 0K), SOECs (C_{ij}) are obtained at required temperature.

$$C_{ij} = C_{ij}^0 + C_{ij}^{vib} \qquad \ldots(6)$$

C_{ij}^0 and C_{ij}^{vib} are SOECs at absolute zero temperature and required temperature, respectively. The detailed expression of C_{11}, C_{12} and C_{44} are given in our previous works[26].

3 Results and Discussion

The SOECs are evaluated in the temperature range 10-70 K using nearest neighbour[12,14] distance (r_0= 3.031Å), hardness parameter[27] (b= 3.313Å) and are presented in Table 1. The temperature dependent ultrasonic velocities for longitudinal and shear modes of propagation along different directions are presented in Table 2. The electrical resistivity values at various magnetic fields 0-15T taken from literature[14] and electronic viscosity computed using Eq. (3) is presented in Table 3. Further, the obtained values of ultrasonic velocities for longitudinal and shear modes of propagation and electronic viscosity are applied to compute ultrasonic attenuation due to EPI along different directions using Eqs (1-2). The ultrasonic attenuation along different directions is presented in Table 3 and shown in Fig. 1.

The elastic constants play vital role to decide mechanical stability and durability of the material. It is obvious from Table 1 that SOECs are varying with small values in the chosen temperature range *i.e.,* 10-70 K, C_{11} and C_{44} increase while C_{12} decrease with increase in temperature. This type of behaviour is similar to previous studies[26,28] and is based on our used formulation to compute SOECs.

The wave velocity is a principal factor in ultrasonic characterization, which can provide imperative tools in understanding the scrutinizing ability of material. Table 2 describes the increase in ultrasonic velocity with increasing temperature for both modes of propagation *i.e.,* longitudinal as well as shear due to SOECs. Ultrasonic velocity for shear mode of propagation along <100> direction (for the polarization along <100>) and <110> direction (for the polarization along <001> direction) is the same due to constant values of shear velocity along these directions as given in literature[22]. Moreover, the ultrasonic velocity for longitudinal mode of propagation is more than that for shear mode. The nature of wave velocity is found to be similar to our previous studies[26,28-30].

Table 1 — SOEC of CeAs in the temperature range 10 - 70 K (10^{10} N/m^2)

Temp (K)	C_{11}	C_{12}	C_{44}
10	4.206	1.076	1.097
20	4.206	1.075	1.097
30	4.207	1.071	1.097
40	4.213	1.065	1.098
50	4.220	1.059	1.098
60	4.230	1.052	1.098
70	4.242	1.048	1.099

The obtained results of ultrasonic attenuation along different crystallographic directions with other two parameters viz. electrical resistivity and viscosity are given in Table 3. Ultrasonic attenuation reduces the defects to be detectable especially in cerium monoarsenide with coarse grains or complex microstructures. Therefore, it is desirable to minimize ultrasonic attenuation in order to maximize the usefulness of ultrasonic computation. Fig. 1 shows that ultrasonic attenuation of CeAs ceases at 30, 40, 50, 60 K for magnetic fields of 0, 2, 5, 10 and 15T, respectively. The value of ultrasonic attenuation increases with increase in magnetic field. The lowest attenuation is obtained at 0T and highest at 15T. It implies that CeAs is more useful in the absence of magnetic field and in the temperature range 10-30 K. It is most prominent at 30 K.

It is also noticeable that ultrasonic attenuation due to EPI along <100> and <110> directions is the same for shear wave polarized along <100> and <001> directions, respectively as presented in Table 3. It is due to the same values of ultrasonic velocity for shear wave mode along <100> and <110> directions, the similar nature and approximately the same values of ultrasonic attenuation in CeAs are obtained along <100> and <110> directions because of the same numerical value of attenuation in these two directions within ±3-4% error. The present results show that the attenuation decreases rapidly as temperature

Table 2 — Ultrasonic velocities (10^3 m/s) of CeAs along different directions in the temperature range 10-70 K

Directions	Velocity	10 K	20 K	30 K	40 K	50 K	60 K	70 K
<100>	V_L	2.574	2.574	2.574	2.576	2.578	2.581	2.584
	V_{S1}=V_{S2}	1.315	1.315	1.315	1.315	1.315	1.315	1.315
<110>	V_L	2.426	2.423	2.426	2.426	2.426	2.427	2.427
	V_{S1}	1.315	1.315	1.315	1.315	1.315	1.315	1.315
	V_{S2}	2.220	2.221	2.223	2.226	2.231	2.237	2.244
<111>	V_L	2.375	2.375	2.374	2.374	2.373	2.373	2.373
	V_{S1}=V_{S2}	1.489	1.489	1.091	1.493	1.495	1.498	1.502

Table 3 — Temperature variation of electrical resistivity, R (Ωm) and electronic viscosity, η_e (10^{-6} kg/ms) of CeAs in the magnetic field range 0-15T

Magnetic field (T)	Temp (K)	R	η_e	$(\alpha/f^2)_{L1}$	$(\alpha/f^2)_{L2}$	$(\alpha/f^2)_{L3}$	$(\alpha/f^2)_{S1}$	$(\alpha/f^2)_{S2}$	$(\alpha/f^2)_{S3}$	$(\alpha/f^2)_{S4}$
0	5	42	1.411	0.342	0.436	0.408	2.570	1.765	2.570	0.533
	20	95	0.623	0.151	0.192	0.180	1.136	0.780	1.136	0.235
	50	825	0.071	0.017	0.022	0.020	0.130	0.088	0.130	0.026
	70	775	0.076	0.018	0.023	0.022	0.139	0.093	0.139	0.028
2	5	40	1.481	0.359	0.457	0.429	2.698	1.854	2.698	0.559
	20	78	0.759	0.184	0.234	0.220	1.384	0.950	1.384	0.287
	50	820	0.072	0.017	0.022	0.020	0.131	0.089	0.131	0.026
	70	775	0.076	0.018	0.023	0.022	0.139	0.093	0.139	0.028
5	5	38	1.559	0.378	0.481	0.451	2.840	1.951	2.840	0.589
	20	56	1.058	0.256	0.326	0.306	1.927	1.323	1.927	0.399
	50	775	0.076	0.018	0.023	0.022	0.139	0.094	0.139	0.028
	70	747	0.079	0.019	0.024	0.022	0.144	0.096	0.144	0.029
10	5	16	3.704	0.898	1.143	1.072	6.747	4.635	6.747	1.399
	20	40	1.481	0.359	0.457	0.429	2.698	1.853	2.698	0.559
	50	640	0.092	0.022	0.028	0.026	0.168	0.114	0.168	0.034
	70	710	0.083	0.020	0.025	0.024	0.151	0.102	0.151	0.030
15	5	13	4.558	1.106	1.407	1.320	8.304	5.704	8.304	1.722
	20	27	2.195	0.532	0.678	0.635	3.998	2.745	3.998	0.829
	50	450	0.131	0.031	0.040	0.038	0.239	0.163	0.239	0.049
	70	650	0.091	0.022	0.028	0.263	0.165	0.111	0.165	0.033

L1: ultrasonic attenuation for longitudinal wave in direction <100>,L2.: ultrasonic attenuation for longitudinal wave in direction <111>,L3: ultrasonic attenuation for longitudinal wave in direction <110>,S1: ultrasonic attenuation for shear wave in direction <100>,S2: ultrasonic attenuation for shear wave in direction <111>,S3: ultrasonic attenuation for shear wave in direction <110>, polarised in <001>,S4: ultrasonic attenuation for shear wave in direction <110>, polarised in <1 $\bar{1}$ 0>

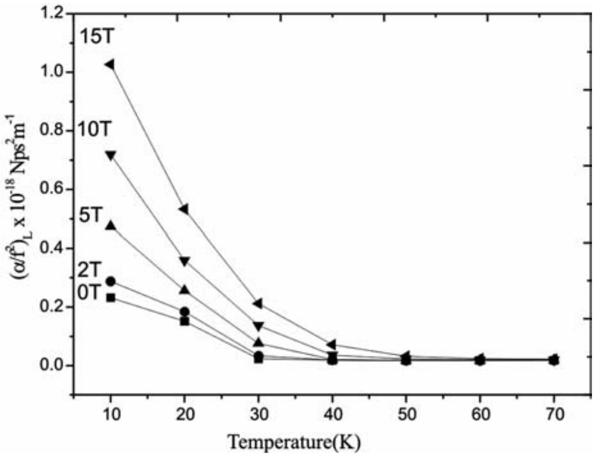

Fig. 1 — $(\alpha/f^2)_L$ along <100> of CeAs versus temperature at various magnetic fields

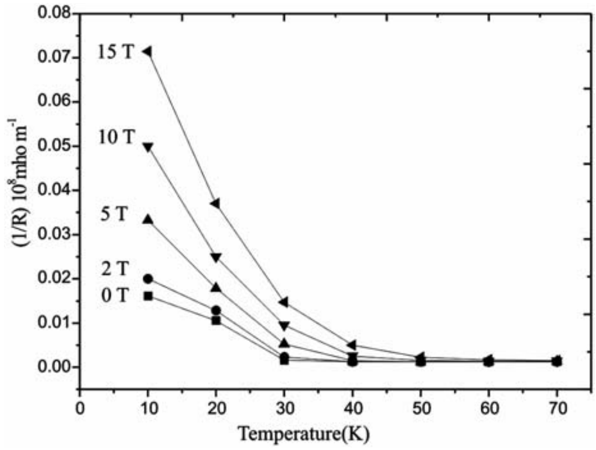

Fig. 2 — $1/R$ versus temperature of CeAs at various magnetic fields

increases. It is also observed from Fig. 1 and Table 3 that ultrasonic attenuation for shear waves is larger than for longitudinal waves because of V_L and V_S values. Further, from Eqs. (1-2) we have, $\alpha \propto 1/V^3$. Thus, $\alpha_L / \alpha_S = V_S^3 / V_L^3$ is satisfied along <100> and <110> directions.

Thus, it may be concluded that ultrasonic attenuation due to EPI for longitudinal and shear waves is analogous to the reciprocal of $(1/V^3)$. There is no experimental data available for CeAs thus we compare our result to other B_1 structured materials. This behaviour is similar to other previous studied materials like neptunium telluride[28], transition metals[29], alkali metals[30], coinage metals[31], vanadium and tungsten[32] and cerium monopnictides[33].

Figure 2 shows a graph between inverse of electrical resistivity ($1/R$) versus temperature for CeAs at magnetic fields 0, 2, 5, 10 and 15T, respectively. By comparing the nature of this particular graph (Fig. 2) with temperature varying ultrasonic attenuation versus temperature as shown in Fig. 1, the similar trend of all these graphs is observed along the three crystallographic directions. Thus, the electrical resistivity plays an important role in determining the nature of ultrasonic attenuation due to EPI. Hence, electrical resistivity is the deciding factor for evaluating ultrasonic attenuation even though there are lot of factors involved in present computation.

4 Conclusions

Simple methods are reported to calculate SOECs, ultrasonic velocities, ultrasonic attenuation due to EPI. Following points may be concluded:

The electrostatic and repulsive (Coulomb and Born-Mayer) potential model is applied successively to evaluate SOECs of CeAs using two basic parameters *i.e.*, the nearest neighbour distance and hardness parameter. The obtained results are found to be in good agreement with previous findings. The ultrasonic velocities of CeAs for longitudinal and shear modes are evaluated along <100>, <110> and <111> directions in the temperature range 10-70 K. The ultrasonic velocity is found to be the highest along <100> and may be used for complete usefulness for cerium monoarsenide. The ultrasonic attenuation due to EPI decreases with increase in temperature. Attenuation is the highest along <100> direction for longitudinal mode of propagation. Thus, it is concluded that <100> direction will be more useful for the application of CeAs. The ultrasonic attenuation due to EPI is higher for shear wave propagation than for longitudinal wave propagation. This is mainly due to greater value of C_{11} than C_{44}. It is observed that at low magnetic field *i.e.*, 0T, the attenuation is low and at high magnetic field *i.e.*, 15T, the attenuation is high. It implies that attenuation is directly proportional to the magnetic field. It is significant at 30 K. The attenuation in CeAs ceases at 30, 40, 50, 60 and 60 K for 0, 2, 5, 10 and 15T, respectively. Hence, the electron mean free path is not equal to phonon mean free path. Thus, no coupling will take place after this temperature at these magnetic fields. The variation of ultrasonic attenuation with temperature is not linear but similar to variation of reciprocal of resistivity ($1/R$) with temperature. Thus, resistivity is also a key factor for deciding the nature of ultrasonic attenuation.

Hence, the electrical and magnetic properties play an important role to characterize cerium arsenide using ultrasonic evaluations. The obtained results of this work definitely support our views on ultrasonic parameters. The ultrasonic parameters are inbuilt belongings of CeAs. The computed parameters help in future implication of CeAs in various practical applications such as in the field of non-linear optics, electronics (spintronics) etc. These results together with other thermophysical properties are very useful for appraisal of future performance of CeAs.

References

1 Miller V, Maurer D, Scheidt E W, Roth C & Lüder K, *Solid Stat Commun,* 57 (1986) 319.
2 Lüthi B & Yoshizawa M, *J Magn Magn Mat* 63-64 (1987) 274.
3 Mishra G, Singh D, Yadawa P K, Verma S K & Yadav R R, *Platinum Metals Rev,* 57 (2013) 186.
4 Bhalla V, Kumar R, Tripathy C & Singh D, Int J Mod Phys, B 27 (2013) 1350116 (28pp).
5 Pandey D K, Singh D, Bhalla V, Tripathi S & Yadav R R, *Indian J Pure & Appl Phys,* 52 (2014) 330.
6 Coban C, Colakoglu K & Ciftci Y O, *Mater Chem Phys,* 125 (2011) 887.
7 Shekar N V C & Sahu P C H, *J Mat Sci,* 41 (2006) 3207.
8 Hulliger F & Ott Z H R, *Eur Phys J B,* 29 (1978) 47.
9 Rainford B, Tuberfield K C, Busch G & Vogt O, *J Phys C Soild State Phys,* 1 (1968) 679.
10 Werner A, Hochheimer H D, Meng R L & Bucher E, *Phys Lett A,* 97 (1983) 207.
11 Svane A, Szotek Z, Temmerman W M, Laegsgaard J & Winter H, *J Phys: Condens Matter*, 10 (1998) 5309.
12 Mori N, Okayama Y, Takahashi H, Kwon Y S & Suzuki T, *J Appl Phys,* 69 (1991) 4696.
13 Nimori S, Kido A, Kido G, Nakagawa Y, Haga Y & Suzuki T, *Physica B,* 186-188 (1993) 173.
14 Mori N, Okayama Y, Takahashi H, Haga Y & Suzuki T, *Physica B*, 186-188 (1993) 444.
15 Thompson J D and Lawrence J M *Handbook of the Physics and Chemistry of Rare-Earths. Lanthanides/Actinides: Physics II* (Amsterdam: Elsevier) Vol. 19 *(eds.)* A Karl, Gschneidner Jr., L R Eyring, G H Lander, G R Choppin (1994) 383.
16 Srivastava V, Bandyopadhyay A K, Jha P K & Sanyal S P, *J Phys Chem Solids*, 64 (2003) 907.
17 Bhardwaj P and Singh S, *Proceedings of the World Congress on Engineering,* Vol III: WCE, London, U.K (2011)
18 Morse R W, *Phys Rev,* 97 (1955) 1716.
19 Kor S K & Yadav R R, *J Pure Appl Ultrason,* 8 (1986) 89.
20 Mason W P, *Phys Rev,* 97 (1955) 557.
21 Mason W P, *Piezoelectric Crystals and Their Applications to Ultrasonics* (Van Nostrand: New York), 1950.
22 Gupta S L & Kumar V, *Solid State Physics*, 9th ed., (Kedar Nath & Co., Meerut), 2012.

23 Kittle C, *Introduction to Solid State Physics*, 8th ed., (Wiley, New Delhi), 2005.
24 Brugger K, *Phys Rev A,* 133 (1964)1611.
25 Leibfried G & Ludwig W, *Theory of anharmonic effect in crystal*, In: Seitz F & Turnbull D, Editors, *Soild State Physics,* (Academic Press, New York), 1966, Vol 12 pp 276-444.
26 Singh D, Pandey D K, Singh D K & Yadav R R, *Appl Acoust*, 72 (2011) 737.
27 Tosi M P, *Solid State Physics* (New York : Academic Press) Vol 16 (*eds.)* F Seitz, D Turnbull 1 (1964)
28 Singh D, Yadawa P K & Sahu S K, *Cryogenics,* 50 (2010) 476.
29 Singh D, Pandey D K, Yadawa P K & Yadav A K, *Cryogenics,* 49 (2009) 12.
30 Yadav R R & Singh D, *J Acoust Soc Ind,* 29 (2001) 220.
31 Kor S K, Kailash, Shanker K & Mehrotra P, *J Phys Soc Japan*, 56 (1987) 2428.
32 Kor S K & Khare R P, *Acustica,* 42 (1979) 179.
33 Yadav R R, Tiwari A K & Singh D, *J Mat Sc,* 40 (2005) 5319.